The mating system of the *Eucalyptus* canker pathogen *Chrysoporthe austroafricana* and closely related species

Aquillah M. Kanzi[1], Emma T. Steenkamp[1], Nicolaas A. Van der Merwe[1] and Brenda D. Wingfield[1]

[1]Department of Biochemistry, Genetics and Microbiology, Forestry and Agricultural Biotechnology Institute, University of Pretoria, Pretoria, South Africa

*corresponding author: aquillah.kanzi@fabi.up.ac.za

Highlights

• Genomes of *C. austroafricana*, *C. deuterocubensis* and *C. cubensis* were sequenced.

• Heterothallism and homothallism predicted in *Chrysoporthe* species.

• *C. austroafricana*, *C. deuterocubensis* and *C. cubensis* have unique *MAT* loci.

• *C. austroafricanaMAT1-2* locus contains a truncated *MAT1-1-1* gene.

• LTRs predicted in the *MAT* loci of *C. deuterocubensis* and *C. cubensis*.

• First characterization of the *MAT* locus among the described *Chrysoporthe* species.

Abstract

Fungi in the genus *Chrysoporthe* are economically important canker pathogens of commercially grown *Eucalyptus* species and native Myrtales. Before the current study, homothallism was widely accepted as the mating system of these species, but this hypothesis could not be fully tested. Using whole genome sequences, we characterized the *MAT* locus of two *C. austroafricana* isolates and its sibling species, *C. cubensis* and *C. deuterocubensis.* A unique *MAT1-2* idiomorph containing a truncated *MAT1-1-1* gene, and a *MAT1-1-2* gene, was identified in one isolate of *C. austroafricana* and a *MAT1-1* idiomorph was found in the other. The presence of a single idiomorph in each isolate suggests that this fungus is heterothallic. Screening for *MAT* genes in 65 *C. austroafricana* isolates revealed a bias towards *MAT1-2* idiomorphs suggesting a recent introduction in *Eucalyptus* species. *Chrysoporthe cubensis* and *C. deuterocubensis* are apparently homothallic since all the expected *MAT* genes were identified in their genome sequences. These findings were corroborated by the expression profiles of pheromone genes and their receptors, which conformed to the expected patterns observed in heterothallic and homothallic isolates. Long terminal repeats (LTRs) and specifically retrotransposons were identified in the *MAT* locus of *C. deuterocubensis and C. cubensis*, indicating that the evolution of mating systems in *Chrysoporthe* species might be mediated by these and other repeat elements.

Keywords: *MAT* locus, *Chrysoporthe*, mating systems, heterothallic, homothallic, retrotransposons

1. Introduction

Chrysoporthe austroafricana and its sibling species, *C. cubensis* and *C. deuterocubensis*, are pathogens of *Eucalyptus* species and other trees in the Myrtales (Gryzenhout et al., 2004; Rodas et al., 2005; van der Merwe et al., 2010; Wingfield et al., 1989). *Chrysoporthe austroafricana* causes cankers at the bases and root collars of eucalypts, while cankers caused by *C. cubensis* and *C. deuterocubensis* are found at varying heights on the stem (Conradie et al., 1990). On native *Syzygium* trees, symptoms include branch dieback, and stem and branch cankers (Heath et al., 2006; Nakabonge et al., 2006). Chrysoporthe canker disease has been successfully controlled through resistance breeding of *Eucalyptus* species, although it is still considered an important threat to tree health in commercial eucalypt forestry establishments (Wingfield, 2003).

Sexual fruiting structures (perithecia) dominate *C. austroafricana* cankers on *Syzygium spp.* (Heath et al., 2006; Myburg et al., 2002; Nakabonge et al., 2006). On *Eucalyptus* cankers, asexual fruiting structures (pycnidia) are commonly observed while perithecia are rare (Nakabonge et al., 2006; Wingfield et al., 1989). In contrast, perithecia are predominant in all cankers caused by *C. cubensis* and *C. deuterocubensis*, irrespective of host (Van Heerden and Wingfield, 2001). Although the genetic basis for sexual reproduction in *Chrysoporthe* is unknown, population genetic work also provides evidence that this form of reproduction occurs in nature. Analyses using microsatellite and VCG data revealed high genetic diversity of *C. austroafricana* in South Africa (Vermeulen et al., 2013), which might be indicative of sexual reproduction.

Sexually reproducing filamentous ascomycetes can broadly be categorized as heterothallic or homothallic (Debuchy et al., 2010). Heterothallic fungal strains require a compatible mating partner to complete the sexual cycle, while homothallic strains can complete the sexual cycle without a compatible mate (Coppin et al., 1997; Kronstad and Staben, 1997). In some filamentous ascomycetes, unusual mating systems have been observed. These include pseudohomothallism in *Podospora anserina* and *Neurospora tetrasperma* (Bidard et al., 2011; Merino et al., 1996), mixed mating systems in *Cryphonectria parasitica* (Marra et al., 2004), mating-type switching in *Ceratocystis fimbriata* and *Saccharomyces cerevisiae* (Haber, 2012; Wilken et al., 2014), and unisexual mating in *Neurospora crassa* and *Huntiella moniliformis* (Glass and Smith 1994; Wilson et al., 2015).

Mating in filamentous ascomycetes is controlled by genes that occupy the mating-type (*MAT*) locus (Debuchy and Turgeon, 2006; Turgeon and Yoder, 2000). The *MAT* locus of heterothallic ascomycetes consists of two dissimilar idiomorphs, namely *MAT1-1* and *MAT1-2* (Kronstad and Staben, 1997; Metzenberg and Glass, 1990). The *MAT1-1* and *MAT1-2* idiomorphs are typically characterized by the presence of *MAT1-1-1* and *MAT1-2-1* genes that encode transcriptional regulatory proteins, with an alpha-box and high mobility group (HMG) domains, respectively (Debuchy and Turgeon, 2006; Debuchy et al., 2010). In homothallic species, the *MAT* locus typically does not contain identifiable idiomorphs (mating-types). Instead, genes associated with both *MAT1-1* and *MAT1-2* idiomorphs are present in the same nucleus, allowing the ability to complete the sexual cycle without a mate. Apart from *MAT1-1-1* and *MAT1-2-1*, other genes have been identified in both *MAT1-1* and *MAT1-2* idiomorphs (Wilken et al., 2017).

The process of sexual reproduction in filamentous ascomycetes begins with attraction of compatible mates, mediated by the pheromone-receptor signaling system (Kim et al., 2012). Two classes of pheromones (*ppg1* and *ppg2*) and receptors (*pre-1* and *pre-2*) have been characterized in both heterothallic and homothallic ascomycetes (Kim and Borkovich, 2004; Kim and Borkovich, 2006; Mayrhofer et al., 2006; Zhang et al., 1998). In heterothallic fungi, the transcription of these genes is mating-type specific, while no specific pattern has been observed in homothallic species (Mayrhofer et al., 2006; Nygren et al., 2012). Despite the different transcription profiles in heterothallic and homothallic species, pheromones and receptor genes are crucial during the sexual cycle (Kim and Borkovich, 2004; Kim and Borkovich, 2006; Lee et al., 2008; Mayrhofer et al., 2006). However, the pheromone-receptor signalling system appears dispensable in some homothallic species (Kim et al., 2008; Wendland et al., 2011).

Some studies suggested homothallism in *C. cubensis* (Hodges et al., 1976; Hodges et al., 1979). Unfortunately, attempts to induce mating in the laboratory have been unsuccessful, leaving the mating systems of *Chrysoporthe* species largely unresolved. In such cases, genome sequencing has played a major role in the description of mating-types and evolutionary studies of mating systems in filamentous fungi (Bihon et al., 2014; Dyer and Paoletti, 2005; Dyer et al., 2003; Galagan et al., 2005). The genomes of *C. austroafricana*, *C. cubensis* and *C. deuterocubensis* have been sequenced (Wingfield et al., 2015a, 2015b), thus presenting an opportunity to determine the genetic basis for mating in *Chrysoporthe* species. Therefore, the aims of this study were, two-fold: (i) to characterize the *MAT loci* of *C. austroafricana*, *C. cubensis* and *C.*

deuterocubensis, and (ii) to determine the expression profiles of pheromone and receptor genes of these three species to complement the identified mating systems. The *MAT loci* of selected species in the *Diaporthales* were used for comparative purposes.

2. Materials and methods

2.1. Genome sequences

For this study, the genomes of *C. austroafricana* isolate CMW2113 (accession number JYIP00000000; Wingfield et al., 2015a), *C. cubensis* isolate CMW10028 (accession number LJCY00000000) and *C. deuterocubensis* isolate CMW8650 (accession number LJDD00000000; Wingfield et al., 2015b) were retrieved from NCBI's GenBank database resource of the National Center for Biotechnology Information (NCBI; http://www.ncbi.nlm.nih.gov). Preliminary analysis of the *MAT* genes and the *MAT* locus was inconclusive thus, re-sequencing was performed for *C. austroafricana* isolate CMW2113, *C. deuterocubensis* isolate CMW8650 and *C. cubensis* isolate CMW10028 to improve the quality of these genome assemblies. Additionally, the genome of the putative *MAT1-1* isolate of *C. austroafricana* CMW6102 was sequenced.

Genomic DNA was isolated from fresh mycelia obtained from *C. austroafricana* isolates CMW6102 and CMW2113 grown in 2% malt extract broth, using a modified phenol-chloroform protocol (Steenkamp et al., 1999). The isolated genomic DNA was assessed for quality by gel electrophoresis (0.8% w/v agarose) and subjected to fluorometric quantification using a NanoDrop spectrophotometer (Thermo Fisher Scientific Inc., Waltham, MA USA). Whole genome sequencing for *C. austroafricana* CMW6102 was done using the Illumina HiSeq platform at Fasteris SA (Geneva, Switzerland). For both isolates, the sequence libraries comprised of two paired-end libraries and one mate-pair library with insert size of 250-350 bp, 550-650 bp, and 3000 bp, respectively. Sequence reads for *C. austroafricana* isolates CMW2113 and CMW6102 were assessed for quality, sanitised by removing linker sequences, homopolymers, and low-quality bases, and assembled using IDBA-UD (Peng et al., 2012). In each case, scaffolding was performed with SSPACE Standard v 3 (Boetzer et al., 2011) using all available sanitised reads.

The genome of *C. deuterocubensis* isolate CMW8650 (GenBank Accession LJDD00000000) and *C. cubensis* isolate CMW10028 (GenBank Accession LJCY00000000) were also re-sequenced. Genomic DNA for these isolates were extracted as described above, and subjected to Single-Molecule Real-time Sequencing [SMRT] (Pacific BioSciences, California, United

States) at Macrogen, Inc. (Seoul, South Korea). This genome was assembled using CANU v 1.5 (Koren et al., 2017), and the quality of the assembly was further improved using PILON v 1.22 (Walker et al., 2014). Quantitative assessment of the completeness of all three genome assemblies was performed using BUSCO v 2.0.1 (Simão et al., 2015). For this analysis BUSCO genes from the Sordariomycetes lineage were used, while *Neurospora crassa* genes were used as references for gene prediction using AUGUSTUS.

2.2. Identification and characterization of the *MAT* locus

The respective MAT1-1-1, MAT1-1-2, MAT1-1-3 and MAT1-2-1 protein sequences of *Cryphonectria parasitica* (*Cryphonectriaceae*) (accession numbers AAK83346.1, AAK83345.1, AAK83344.1, and AAK83343.1) were obtained from the GenBank database. Using CLC Genomics Workbench v 9.1 (CLC Bio, Arhus, Denmark), homologs of *C. parasitica MAT* genes were identified from the draft genome sequences of *C. austroafricana* isolates CMW2113 and CMW6102 using the tBLASTx variant of BLAST (Altschul et al., 1990). *APN2* and *SLA* genes, which are commonly associated with *MAT* loci (Rydholm et al., 2007; Wilken et al., 2017), were also used to identify putative *MAT* loci. Similarly, the *C. parasitica MAT* genes were used to query the *C. cubensis* and *C. deuterocubensis* genomes for homologous sequences. Reciprocal tBLASTx was performed to confirm the identified *MAT* homologs. Only sequence hits with at least 50% coverage and E-values of 1E-4 were considered. To annotate the *MAT* containing contigs, open reading frames (ORFs) were predicted using CLC Genomics Workbench and AUGUSTUS v3.0.3 (Stanke and Morgenstern, 2005). FGENESH+ (http://linux1.softberry.com/) was used to confirm the predicted mRNA sequences using respective *C. parasitica MAT* protein sequences as references. The predicted gene models were functionally characterized using BLASTp against the NCBI GenBank database using default BLAST parameters. Conserved domains associated with *MAT* genes were identified and characterized using pfam (http://pfam.xfam.org/) and InterPro (https://www.ebi.ac.uk/interpro/search/sequence-search) protein domain databases with default parameters.

2.3. Evolutionary analysis of *MAT* genes

The phylogenetic relationships of *Chrysoporthe* species using *MAT* gene sequences were determined using maximum likelihood (ML) as implemented in RAxML v 8.2.4 (Stamatakis, 2014). These analyses also included the *MAT* genes of selected species in the *Diaporthales*, including *C. parasitica, Valsa mali* (Yin et al., 2015), *Diaporthe ampelina* (Morales-Cruz et

al., 2015), *Diaporthe longicolla* (Li et al., 2015), *Diaporthe* sp. (Kanematsu et al., 2007), *Melanconium* sp. (Lamprecht et al., 2011), *Lollipopaia minuta* (Inderbitzin and Berbee, 2001) and *Phaeoacremonium aleophilum* (Blanco-Ulate et al., 2013). Multiple sequence alignments of the *MAT* genes were generated using MAFFT v 7.182 (Katoh et al., 2002) and visualized in CLC Genomics Workbench. Multiple sequence alignments were trimmed to remove poorly aligned regions using trimAl (Capella-Gutierrez et al., 2009). Sequences from *Acidothrix acidophila* (Hujslová et al., 2014) and *Magnaporthe grisea* (Kanamori et al., 2007) were used to root the trees. Additionally, for comparison of tree topologies, a reference tree was generated using 185 single copy protein sequences (Supplementary Table 3) identified using BUSCO (Simão et al., 2015). Nodal support values were determined using 1000 bootstrap replicates. To gain insight into the evolution of the *MAT* locus in the *Diaporthales*, structures of previously characterized *MAT* loci were retrieved from GenBank or determined from the available whole genome sequences and mapped onto the generated reference tree.

2.4. PCR amplification of *MAT* genes of *C. austroafricana* isolates

PCR amplification was performed to provide molecular evidence for the presence of *MAT* genes. Also, using these primers, the distribution of *MAT* genes in a population of *Chrysoporthe* isolates was determined by PCR amplification. To achieve this, sequence-specific primer pairs were designed to amplify fragments of putative *MAT* genes (Fig. 1B) identified from the genomes of *C. austroafricana* isolates CMW2113 and CMW6102. Sequence alignments for primer design included *MAT* genes of *C. austroafricana* (CMW2113 and CMW6102), *C. cubensis* and *C. deuterocubensis*. Primers were designed using Primer3 (http://primer3.ut.ee/) and CLC Genomics Workbench v 8.0.1, and synthesized at Inqaba Biotec (Pretoria, South Africa). The primers were optimized for PCR using isolates from which *MAT* genes were identified. Genomic DNA was extracted as previously described from seven-day old cultures of 65 *C. austroafricana* isolates (Supplementary Table 2). PCR reactions to amplify portions of putative *MAT* genes included 40 ng DNA, 2.5 μl 10 x PCR reaction buffer with $MgCl_2$, 0.5 μM of each primer, 1 U Kapa *Taq* polymerase (Kapa Biotech, South Africa), and sterilized distilled water to a total volume of 25 μl. DMSO (2.5 μl) was included in the PCR reaction to amplify portions of the *MAT1-1-1* and *MAT1-1-2* gene. Standard PCR conditions were used for all reactions with annealing temperatures for each specific primer pair obtained from primer synthesis reports. To test the null hypothesis that the frequency of *MAT1-1* to *MAT1-2* is 1:1, a chi-square test was used at $P = 0.05$ significance level.

Table 1: Primers used to amplify portions of *MAT* genes characterized in this study.

Primer	Primer sequence (5' -3')	Annealing temp.(°C)	Region amplified	Amplicon size
acdmat121F	AACCGTCTTCTTGTTGGTC			
acdmat121R	GTGGTAGTCTTCTTGGAACG	59°C	*MAT1-2-1*	536 bp
acdmat111F	CGGGTGTGGACGTTTATC			
acdmat111R	CCGATCTCATCAAACGCC	60°C	*MAT1-1-1*	842 bp
acdmat112	TTGAAAGCAACMCTGACCGA			
acdmat112	GCCGTGGAGAATATGCAGAA	60.4°C	*MAT1-1-2*	912 bp
mat113qF	TTCATCATTGCACGTACCGA			
acdmat113R	GTACTTTGCTTGGTGTTGAT	58.4°C	*MAT1-1-3*	467 bp

* Temperature
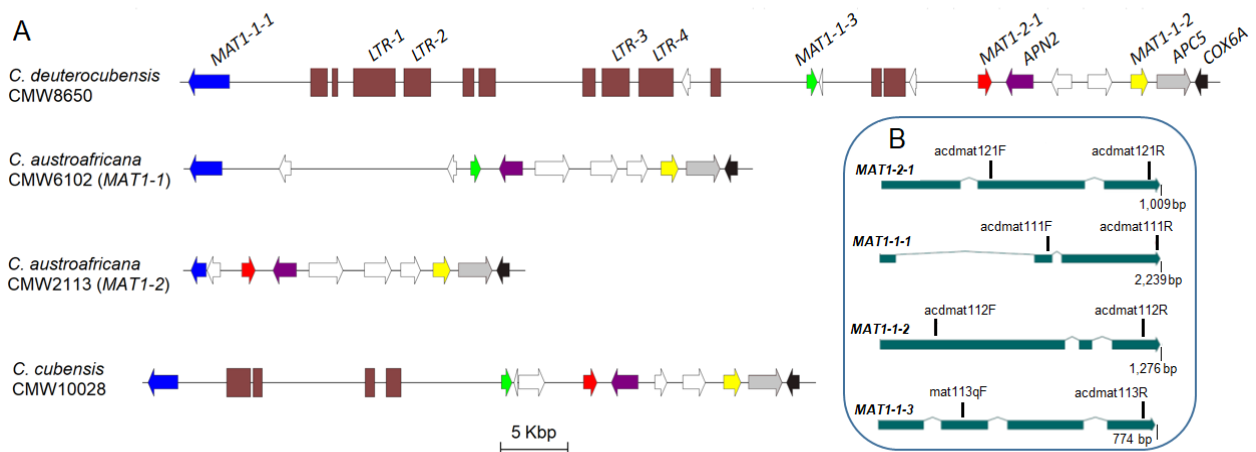
Fig. 1. (A) *MAT* loci of *C. austroafricana* CMW6102 (*MAT1-1*), *C. austroafricana* CMW2113 (*MAT1-2*), *C. deuterocubensis* and *C. cubensis* showing genes and repeat regions. (B) Annotation of the diagnostic *MAT* primers on the *MAT* genes of *C. cubensis*. The location of the *MAT* gene primers was the same in *C. austroafricana*, and *C. deuterocubensis*.

2.5. Identification and characterization of pheromone and pheromone receptor genes

The *C. parasitica* α-like pheromone gene *Mf1-1* (similar to *ppg-1* of other ascomycetes) (GenBank accession no. AAC39328) and the a-like pheromone gene *Mf2-1* (similar to *ppg-2* of other ascomycetes) (GenBank accession no. AAC39329) (Zhang et al., 1998) were used to

query the whole genome sequence of the newly assembled genomes of *C. austroafricana* (isolates CMW2113 and 6102), *C. deuterocubensis* and *C. cubensis* (Wingfield *et al.* 2015b) using tBLASTn in CLC Genomics Workbench 8.0.1 (CLC Bio, Arhus, Denmark). In all three *Chrysoporthe* species, the pheromone receptor genes (*pre-1* and *pre-2*) were identified by searching for protein sequences containing conserved transmembrane domains in the InterPro database (https://www.ebi.ac.uk/interpro/interproscan.html). Protein sequences homologous to *pre-1* and *pre-2* of other filamentous ascomycetes were identified by BLASTp searches against the protein sequence database in NCBI.

2.6. Transcription analysis of *MAT1*, pheromone and receptor genes

For gene expression analysis, *C. cubensis* isolate CMW10028 was used to represent homothallic strains, while two *C. austroafricana* individuals of opposite mating-type (isolate CMW2113 (*MAT1-2*) and isolate CMW6102 (*MAT1-1*) were used. Inoculums of *C. austroafricana* CMW2113, *C. austroafricana* CMW6102 and *C. cubensis* were transferred from actively growing mycelia in 2% w/v malt extract agar plates into respectively labelled 250 ml conical flasks containing 100 ml of 2% w/v malt extract broth. The three isolates were incubated for four days at 25°C in the dark with shaking at 150 rpm. For each isolate, mycelia were harvested by filtration through sterilized Whatman® qualitative filter paper, grade 1 (Sigma-Aldrich, St. Louis, USA). Total RNA was extracted using the RNeasy Plant Mini Kit (Qiagen, Hilden, Germany). Freshly isolated fungal mycelia were frozen using liquid nitrogen and ground to a fine powder using a mortar and pestle. Approximately 100 mg of the ground mycelia was used for a single extraction mix. For this extraction, 10 μl/ml of *β*-mercaptoethanol was added into the RLC lysis buffer, containing high concentrations of guanidine hydrochloride. The extracted total RNA was quantified using a Qubit 2.0 instrument (Thermo Fisher Scientific Inc., Waltham, MA USA) and stored at -80°C. Using 100 ng of total RNA per sample, cDNA synthesis was performed using the SuperScript IV Reverse Transcriptase kit (Thermo Fisher Scientific Inc., Waltham, MA USA) following the manufacturer's protocol. The Oligo d(T)20 primer was used for this reaction. Excess RNA was removed from the synthesized cDNA by RNase H treatment and the final product was diluted 1:2 with RNAse free water.

The quantitative reverse transcription PCR (RT-qPCR) assay was performed in three technical replicates on a QuantStudio™ 12K Flex thermal cycler (Applied Biosystems). The primers used for this assay (Table 2) were designed using CLC Genomics Workbench and synthesized at Inqaba Biotec (Pretoria, South Africa). These primers specifically targeted the pheromone

(*ppg1* and *ppg2-1*) and pheromone receptor (*pre-1* and *pre-2*) genes, as well as the genes encoded at the mating-type locus (i.e., *MAT1-1-1*, *MAT1-1-2*, *MAT1-1-3* and *MAT1-2-1*). The relative expression for the genes was calculated using the comparative CT (threshold cycles) method (Schmittgen and Livak, 2008), with the single copy actin gene as an internal reference (Karlsson *et al.* 2008). Statistical differences in gene expression were calculated using one-way analysis of variance (ANOVA) in the R 3.2.2 statistical package.

Table 2: Oligonucleotide sequences used as Primers for RT-qPCR analysis of mating-type, pheromone and pheromone receptor genes of *Chrysoporthe austroafricana*, *C. deuterocubensis* and *C. cubensis*.

Gene	Primer ID	Primer sequence (5'-3')	temp (°C)
pre-1	pre1Q1_L	GCTCTTGAACATCCGTCTC	62.5 °C
	pre1Q1_R	TAGTCTCCTTGGTGGTGGT	
pre-2	pre2Q1_L	GACAATGACACCGAAGACC	62.5 °C
	pre2Q1_R	CCAGGAGGAGTTGAAGTAGAC	
ppg	cappg1Q1L	CCGAGATCTCCAACATGCG	62.5 °C
	cappg1Q1R	CCGAACTTGGACAGGATGG	
ppg2	ppg2Q1_L	TCTTCCTCCTCATCCACGTC	62.5 °C
	ppg2Q1_R	CTGCAGAGCTGCAAAGAGG	
actin	actQ_L	GTCGTGACTTGACCGACTAC	62.5 °C
	actQ_R	GCAGAGCTTCTCCTTGATGT	
MAT1-1-1	mat1QL	CTGGACGACTTCACGCTG	62.5 °C
	mat1QR	CATGACGTGCAGGCTGTG	
MAT1-2-1	mat2QL	TCTCATTGTCACCGATGCTG	62.5 °C
	mat2QR	GGTCTGGTTGGCAGGAAG	
MAT1-1-2	mat112QL	CGCATGGCAAATTCCTTGTC	62.5 °C
	mat112QR	TGGACGATGTCGTGTTGAAG	
MAT1-1-3	mat113QL	TTCATCATTGCACGTACCGA	62.5 °C
	mat113QR	AGTTGAGGCTGATCTTGTCG	

3. Results

### 3.1. Sequencing and assembly of *C. austroafricana* and *C. deuterocubensis* genomes

Illumina whole genome sequencing of *C. austroafricana* CMW6102 generated approximately 8.5 GB and 10.2 GB of paired-end and mate-paired reads, respectively. Re-sequencing of *C. austroafricana* CMW2113 produced approximately 9 GB of paired-end reads and 11 GB of mate-paired reads. *De novo* assembly of the *C. austroafricana* CMW2113 genome resulted in

an assembly of approximately 48 MB that was comprised of 2961 contigs, with an N50 of 130905. After scaffold assembly, 227 scaffolds over 200 bp with an N50 of 5,060,702 bp were recovered. This whole genome shotgun project has been deposited at DDBJ/EMBL/GenBank under the accession JYIP00000000. The version described in this paper is version JYIP02000000. The *de novo* assembly of the *C. austroafricana* CMW6102 genome also resulted in an assembly of 48 MB comprised of 3319 contigs (N50 = 64824 bp) that were further simplified to 150 scaffolds (N50 = 3,033,680 bp) over 200 bp. This whole genome shotgun project has been deposited at DDBJ/EMBL/GenBank under the accession PKSD00000000. The version described in this paper is version PKSD01000000. SMRT sequencing of *C. deuterocubensis* generated three libraries of approximately 20 GB each, containing reads of at least 20 kb in length. *De novo* assembly of the *C. deuterocubensis* genome generated a 47 MB assembly comprised of 44 contigs with an N50 of 4,135,604 bp and approximately 38x average coverage. This genome has been deposited at DDBJ/EMBL/GenBank under the accession LJDD00000000. The version described in this paper is version LJDD02000000. As for *C. cubensis*, SMRT sequencing generated three libraries of approximately 10 GB each. The average length of the reads in each of the libraries was approximately 10 kb. *De novo* assembly using CANU generated a genome of approximately 44 Mb containing 88 contigs with a N50 of 3,280,246 bp and an average coverage of 36x. This genome was deposited at DDBJ/EMBL/GenBank under the accession number LJCY00000000. The version described in this paper is version LJCY02000000. BUSCO analysis revealed that the *C. austroafricana* CMW2113, *C. austroafricana* CMW6102, *C. deuterocubensis* CMW8650 and *C. cubensis* CMW10028 genomes were 93.1%, 93.9%, 96.1% and 96.5% complete, respectively.

3.2. Identification and characterization of the *MAT* locus

Sequence homologs of *C. parasitica MAT1-1-1*, *MAT1-2-1* and *MAT1-1-2* genes were identified on scaffold7; JYIP02000007.1 (4.59 Mb) of *C. austroafricana* isolate CMW2113 in regions where putative ORFs were predicted using AUGUSTUS (Fig. 1A). In *C. austroafricana* isolate CMW6102, ORFs with sequences homologous to *C. parasitica MAT1-1-1*, *MAT1-1-2* and *MAT1-1-3* were identified on scaffold6; PKSD00000006.1 (3.1 Mb), but genomic regions homologous to *MAT1-2-1* could not be identified (Fig. 1A). Apart from *MAT* genes, ORFs homologous to DNA lyase (*APN2*), *APC5*, and *COX6A* genes, which are commonly associated with the *MAT loci* of filamentous ascomycetes (Turgeon 1998), were identified on the scaffold(s) containing *MAT* genes in *C. austroafricana* isolates CMW2113

and CMW6102 (Fig. 1A). *APN2, APC5* and *COX6A* were within the *MAT loci* of both *C. austroafricana* CMW2113 and CMW6102. In isolate CMW2113, the *SLA2* gene was identified approximately 312 kb upstream of the putative *MAT1-1-1* gene on the same scaffold, while in isolate CMW6102 it was identified on a separate scaffold. Based on *MAT* gene content and organization, *C. austroafricana* isolates CMW2113 and CMW6102 were respectively designated as *MAT1-2* and *MAT1-1* mating-types, consistent with heterothallism. Pairwise sequence comparison of the *C. austroafricana MAT loci* using BLASTn revealed long stretches of syntenic sequence blocks, but dissimilarity was observed in the genomic region between *APN2* and *MAT1-1-1* (Fig. 2), which is consistent with the general structure of *MAT1* idiomorphs (Coppin et al. 1997).
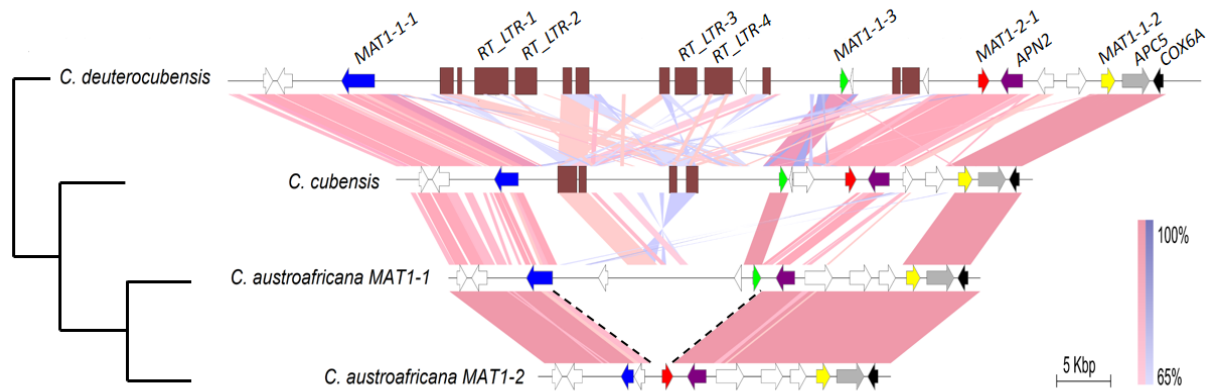
Fig. 2. Synteny comparison of *MAT* loci of *C. austroafricana* CMW6102 (*MAT1-1*), *C. austroafricana* CMW2113 (*MAT1-2*), *C. deuterocubensis* and *C. cubensis*. Syntenic blocks of over 200 nucleotide are shown. Dotted lines between the *C. austroafricana* CMW2113 and CMW6102 *MAT* loci indicate the predicted idiomorphic region. Synteny maps were generated using Easyfig 2.2.2 (Sullivan et al. 2011).

The *MAT1-2* idiomorph (*C. austroafricana* CMW2113) contained a putative *MAT1-1-1* gene that was 1,140 bp in size and contained one intron (66 bp). BLASTp analyses of the deduced 358 amino acid protein sequence in pfam did not yield any result, but the α1 HMG box domain was identified using InterPro. When this protein sequence was aligned with other MAT1-1-1 protein sequences, a truncation of 19 amino acids (57 bp) was observed (Supplementary Fig. 1) in the alpha box domain. The putative *MAT1-2-1* gene (1,008 bp) contained two introns (60 bp and 69 bp), one of which was predicted at the same position as in *C. parasitica* (Supplementary Fig. 2). BLAST searches against NCBI, pfam and InterPro confirmed the presence of the conserved HMG box domain. The predicted *MAT1-1-2* gene (1,276 bp)

contained two introns (67 bp and 90 bp) and encoded a 372 amino acid sequence containing the typical PPF residues (Supplementary Fig. 4) identified in the MAT1-1-2 protein sequence of *Diaporthe* species and other filamentous fungi (Kanematsu *et al.* 2007). In the *MAT1-1* isolate (*C. austroafricana* CMW6102), the putative *MAT1-1-1* gene (2,416bp) contained two introns (1,123 bp and 66 bp) and encoded a 409 amino acid sequence. The presence of the conserved MAT α1 HMG box domain in *MAT1-1-1* genes was confirmed by BLASTp, pfam and InterPro searches (Supplementary Fig. 1). Putative *MAT1-1-3* (775 bp) and *MAT1-1-2* (1,276 bp) genes contained three (48 bp, 55 bp and 66 bp) and two (67 bp and 90 bp), introns respectively. The conserved HMG domain and PPF motif were present in the deduced 201 and 372 amino acid sequences respectively (Supplementary Figs. 3 and 4).

In *C. deuterocubensis*, intact ORFs homologous to *C. parasitica MAT1-1-1*, *MAT1-1-2*, *MAT1-1-3* and *MAT1-2-1* genes were identified on scaffold1; LJDD02000001.1. The *APN2* commonly associated with the *MAT* locus of filamentous fungi was identified flanking the *MAT1-2-1* gene. However, the *SLA2* gene was identified approximately 262,100 bp upstream of *MAT1-1-1*. The putative *MAT1-1-1* gene (3,065 bp) contained two introns (1,826 bp and 171 bp) and encoded 356 amino acids. BLAST searches against InterPro and pfam confirmed the presence of a conserved MAT α1 HMG box domain in the predicted MAT1-1-1 amino acid sequence (Supplementary Fig. 1). The predicted *MAT1-2-1* gene (1,009 bp) contained two introns (61 bp and 69 bp) at conserved positions, and encodes 292 amino acids. The putative *MAT1-1-3* gene of *C. deuterocubensis* (774 bp) contained three introns (48 bp, 54 bp and 66 bp) at conserved positions and encodes a 201 amino acid long protein. The predicted *MAT1-1-2* gene of *C. deuterocubensis* (1,276 bp) contained two introns (64 bp and 90bp) at conserved positions. The deduced 373 amino acid sequences. BLAST searches against pfam, InterPro and NCBI databases identified conserved HMG box domains in the predicted MAT1-2-1 and MAT1-1-3 and a PPF domain in the predicted MAT1-1-2 (Supplementary Figs. 2, - 4 respectively).

In the *C. cubensis* genome, sequence regions homologous to *MAT1-1-1, MAT1-1-2, MAT1-1-3* and *MAT1-2-1* were located on one scaffold (tig00000003). Like in *C. deuterocubensis*, the *SLA2* gene was identified approximately 225,460 bp upstream of the predicted *MAT1-1-1* gene. The predicted *MAT1-1-1* gene (2,239 bp) of *C. cubensis* contained two introns (1,105 bp and 75 bp) and coded for 353 amino acids. The conserved MAT α1 HMG box domain in the predicted MAT1-1-1 was confirmed by BLAST searches against InterPro and pfam (Supplementary Fig. 1). The putative *MAT1-2-1* gene (1,008) contained two introns (60 bp and

69 bp) at conserved positions. The predicted MAT1-2-1 protein sequence 292 amino acids long and contained the conserved HMG identified by BLAST searches in Pfam and InterPro protein domain databases (Supplementary Fig. 2). The putative *MAT1-1-3* gene (802 bp) contained three introns (48 bp, 55 bp and 66 bp) at conserved positions and encoded a 201 amino acids long protein sequence containing the conserved HMG domain (Supplementary Fig. 3). The predicted *MAT1-1-2* gene (1,275 bp) contained two introns (66 bp and 90bp) at conserved positions. BLAST search in Pfam Interpro and NCBI databases confirmed that the predicted 372 amino acid sequences contained the conserved PPF residues (Supplementary Fig. 4).

In the *MAT* locus of *C. deuterocubensis*, three ORFs that were homologous to long terminal repeat (LTR) retrotransposons were identified between the *MAT1-1-1* and *MAT1-1-3* genes (Fig. 1A). BLASTp results showed that the first ORF (LTR-1) contained five domains, including RT_LTR (cd01647), RNAse_HI_RT_Ty3 (cd09274), RVT_1 (pfam00078), CHROMO (pfam00385) and RVE (pfam00665). The second and third ORFs (LTR-2 and LTR-3) contained a retrotrans_gag domain (pfam03732) from LTR retrotransposons. The fourth ORF (LTR-4) contained three domains, namely RT_LTR (cd01647), RNAse_HI_RT_Ty3 (cd09274) and RVT_1 (pfam00078). All these domains in the three ORFs are associated with reverse transcriptase long repeat transposons (RT-LTRs) that are known to occur in fungal genomes (Gioti et al., 2012; Li et al., 2013). Other sequences homologous to LTRs were identified, but the complete ORFs could not be predicted (Fig. 1A). Further analysis using CENSOR [https://www.girinst.org/censor/index.php] (Kohani et al. 2006) identified fragments of transposable elements in the *MAT* loci of *C. austroafricana* CMW2113 (*MAT1-2* idiomorph), *C. cubensis* and *C. deuterocubensis* (Supplementary Table 1). Interestingly, no transposable elements were identified in the *MAT* locus of *C. austroafricana* CMW6102 (*MAT1-1* idiomorph). A closer look into the predicted LTRs revealed that most were incomplete or partial matches to respective conserved LTR domains. The *C. deuterocubensis MAT* locus had the most LTR fragments predicted (Supplementary Table 1) with only four of these encoding complete ORFs. Incomplete and partial LTR matches were identified in the *C. cubensis* and *C. austroafricana MAT* loci (Supplementary Table 1). Analysis of the *MAT* locus of these three species for repeat induced point (RIP) mutation revealed elevated levels of RIP in the idiomorphic region of the *MAT* locus. The idiomorphic region is where LTRs were predicted in *C. deuterocubensis*, *C. cubensis* and *C. austroafricana* CMW2113. Additionally, the GC content in the idiomorphic region and other regions in the *MAT* locus that were dissimilar was significantly lower that regions which were highly conserved (Supplementary

Fig. 5).

3.3. Evolutionary analysis of *MAT* genes

The predicted MAT1-1-1 amino acid sequences of *C. austroafricana* CMW2113 (*MAT1-2*) and *C. austroafricana* CMW6102 (*MAT1-1*) shared 95% identity (Supplementary Table 1), while the predicted MAT1-1-1 amino acid sequences of *C. cubensis* and *C. deuterocubensis* shared 93% sequence identity. These sequences share approximately 71% sequence identity with the predicted MAT1-1-1 sequences of both *C. austroafricana* isolates. Pairwise comparisons of the predicted *C. austroafricana* CMW2113 MAT1-2-1 amino acid sequences revealed 97% sequence identity with *C. cubensis* and *C. deuterocubensis* respectively (Supplementary Table 2). Sequence comparison of the predicted *C. austroafricana* CMW6102 MAT1-1-3 amino acid sequences revealed 95% and 98% sequence identity with *C. cubensis* and *C. deuterocubensis*, respectively, and absolute conservation of the HMG domain. The predicted MAT1-1-2 amino acid sequences of *C. cubensis* and *C. deuterocubensis* shared 98% sequence identity, and 97% and 96% sequence identity, respectively, with *C. austroafricana* MAT1-1-2. When the *MAT* genes of *Chrysoporthe* species were compared to selected species of *Diaporthales*, lower sequence identities were observed (Supplementary Table 2).

The maximum likelihood phylogenies generated from putative *MAT1-1-1*, *MAT1-1-2*, *MAT1-1-3* and *MAT1-2-1* genes grouped the *Chrysoporthe* species in a single clade, confirming the orthology of these genes (Fig. 3). The *Chrysoporthe* species grouped together in a single clade was well supported >90 % bootstrap all *MAT* gene phylogenies. Due to the short branch lengths observed in the *MAT1-1-2*, *MAT1-1-3* and *MAT1-2-1* phylogenies the exact phylogenetic relationship of the *Chrysoporthe* species could not be determined. However, the *MAT1-1-1* tree was largely congruent with the species tree (Fig. 3). Short branch lengths were also present in the *Chrysoporthe* clade in the reference tree generated from 185 genes. In the *MAT1-1-1*, *MAT1-1-3* and *MAT1-2-1* ML phylogenies, the placement of other species in the *Diaporthales* was consistent with that observed in the reference tree. However, in the *MAT1-1-2* tree, the phylogenetic relationships of *Diaporthe* spp. and *Melanconium* sp. was different to that of the reference tree.
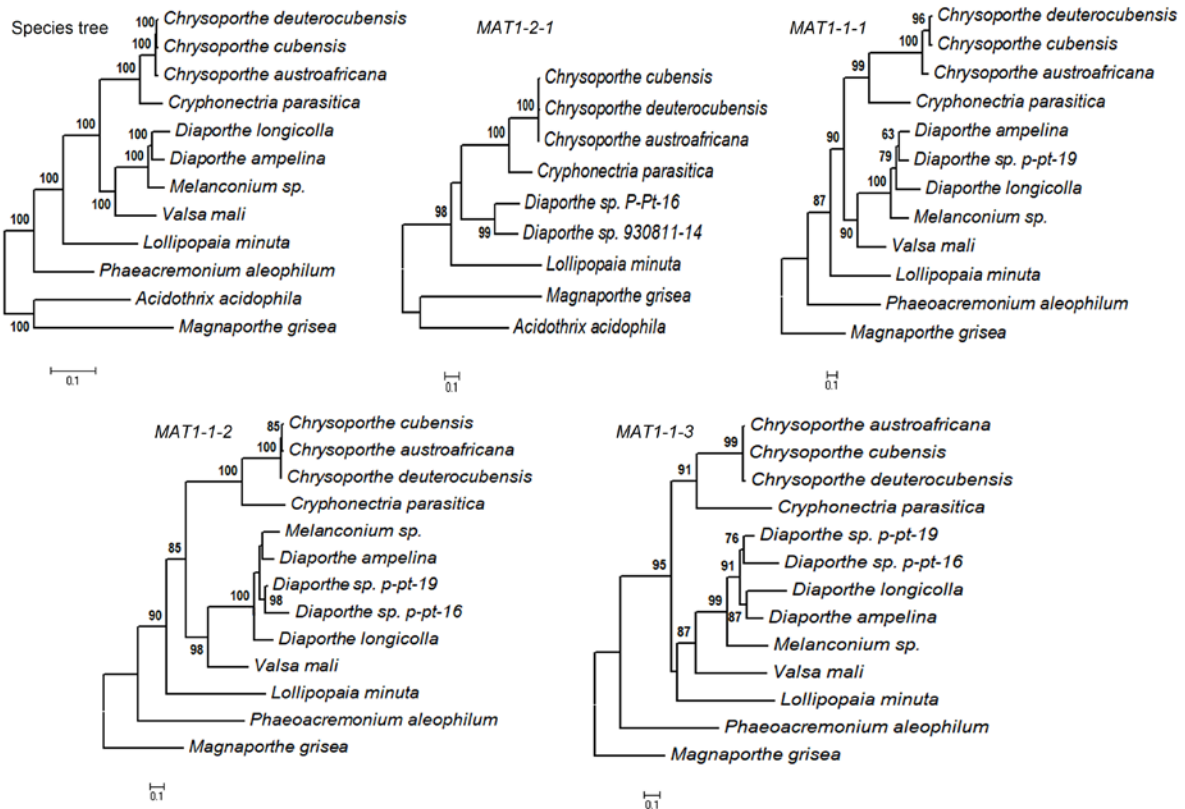
Fig. 3. Maximum likelihood (ML) phylogenetic relationships of *Chrysoporthe* species and other species in the *Diaporthales* using *MAT* genes. The species tree was generated using a concatenated data set of 185 single copy genes (130,492 amino acid characters) while Coding sequences were used for *MAT1-2-1* (546 characters), *MAT1-1-1* (706 characters), *MAT1-1-2* (905 characters) and *MAT1-1-3* (496 characters). The LG + G and GTR + G model of evolution was used in the ML analysis of the species and *MAT* gene phylograms respectively.

The *MAT1-1* loci of *Chrysoporthe* species and other species in the *Diaporthales* were mapped onto the reference tree (Fig. 4). Results from this comparison revealed that the *MAT1-1* locus of *C. austroafricana* CMW6102 was similar in gene content to that of *MAT1-1* idiomorphs of species in the *Diaporthales*, e.g. *C. parasitica*, *V. mali*, *D. ampelina*, *D. longicolla*, *Diaporthe* sp. P-Pt-19, *Melanconium* sp., *L. minuta* and *P. aleophilum*, which contained *MAT1-1-1*, *MAT1-1-2* and *MAT1-1-3* genes. The structure and organization of the *MAT1-1* locus in all these species was highly conserved and syntenic (Fig. 4). Similar to the *C. austroafricana* CMW2113 *MAT1-1* locus, the *MAT1-2* idiomorph of *Diaporthe* sp. P-Pt-16 (accession no. AB199324) contained genes associated with the *MAT1-1* idiomorph, i.e. *MAT1-1-2* and *MAT1-1-3* (Kanematsu et al., 2007). However, the *C. austroafricana MAT1-2* locus contained sequences homologous to *MAT1-1-1* and not *MAT1-1-3*. Among the *Diaporthales* analyzed in

this study, the typical structure of *MAT1-2* idiomorphs (Coppin et al., 1997) was only observed in the *C. parasitica MAT1-2* idiomorph, which contained *MAT1-2-1* only (Fig. 4). The *MAT* locus of *L. minuta* contained all *MAT* genes closely flanked by *APN1* and *SLA2* genes, which was consistent with the typical *MAT* locus of other fungi. Across the *Diaporthales* phylogeny, mating-type gene content consistent with both homothallism and heterothallism was observed.
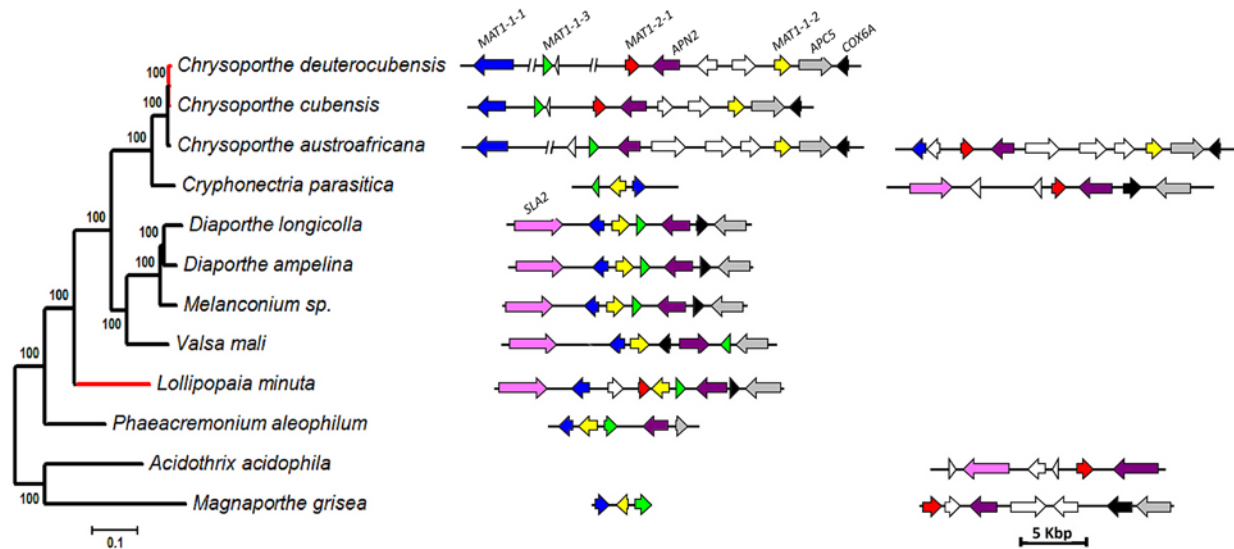
Fig. 4. Comparison of the gene organization in the *MAT* loci of species in the *Diaporthales*. *Magnaporthe grisea* and *Acidothrix acidophila* were used to root the phylogenetic tree. Branches in red show species with a homothallic mating strategy while black branches show species with a heterothallic mating strategy. *MAT1-1* and *MAT1-2* loci for the heterothallic species are shown at the center and on the far right of the figure respectively.

3.4. PCR amplification of *MAT* genes of *C. austroafricana* isolates

The primer pairs designed to amplify portions of *MAT* genes were successfully optimized in *C. austroafricana* (CMW2113 and CMW6102) and sibling species *C. cubensis* (CMW10028) and *C. deuterocubensis* (CMW8650) isolates (Supplementary Fig. 6). Fragments of *MAT1-1-1*, *MAT1-2-1* and *MAT1-1-2* genes were amplified from *C. austroafricana* isolate CMW2113. On the other hand, fragments of *MAT1-1-1*, *MAT1-1-2* and *MAT1-1-3* were amplified from *C. austroafricana* isolate CMW6102. These results were consistent with the gene predictions at the *MAT loci* of *C. austroafricana* isolates CMW2113 and CMW6102 (Fig. 1). Thus, these isolates were designated *MAT1-2* and *MAT1-1* respectively. Testing for *MAT* genes using PCR amplification in a random sample of 65 *C. austroafricana* isolates showed a similar pattern. Fragments of *MAT1-1-1*, *MAT1-1-2* genes were amplified in all isolates while *MAT1-1-3* gene

fragments were amplified from 17 isolates. Fragments of *MAT1-2-1* genes were amplified from 48 isolates, suggesting the presence of both *MAT1-1* and *MAT1-2* idiomorphs in natural populations (Supplementary Table 3). Among the isolates collected from non-native hosts (*Eucalyptus* spp.), the ratio of *MAT1-1/MAT1-2* was 2.75 which calculated to a X^2 value of 6.53 and $P = 0.011$. On the other hand, the ratio of *MAT1-1/MAT1-2* in a population of isolates collected from native hosts (*Syzygium* spp.) was 2.88. Chi-square analysis revealed a X^2 value of 8.26 and $P = 0.004$. This analysis indicated that the null hypothesis of a *MAT1-1/MAT1-2* ratio of 1:1 could be rejected.

3.5. Identification and characterization of pheromone and pheromone receptor genes

3.5.1. ppg1 and ppg2

An ORF homologous to *Mf1-1* of *C. parasitica* (encoding the α-like pheromone) was identified from the genomes of *C. austroafricana* and closely related *C. cubensis* and *C. deuterocubensis.* This ORF was named *ppg1* in accordance to homologous sequences in other *Sordariomycetes.* The putative *ppg1* gene was 1,380 bp (459 amino acids) long in *C. austroafricana* and *C. deuterocubensis*, and 1,383 bp (460 amino acids) in *C. cubensis*. No introns were predicted in any of the putative *ppg1* genes. These genes contained ten repeats of a decapeptide motif (WCLFHGEGCW) that was 100% identical to the mature peptide of *C. parasitica* (Fig. 5). The putative *ppg1* amino acid sequences of *C. austroafricana*, *C. cubensis* and *C. deuterocubensis* contained cleavage sites for Ste13p, which is usually characterized by dipeptide repeats of XP, XA, or XR on the N-terminal end, and cleavage sites for Kex2p consisting of KR or KX on the C-terminal end of each decapeptide motif (Bobrowicz et al., 2002; Pöggeler, 2000). From the sequence alignment the Ste13p cleavage sites included DP, DA or EA, which immediately preceded the mature decapeptide. The identified *Kex2* cleavage site (KR) immediately bordered the mature decapeptide motif, but in some instances the cleavage site was preceded by KE, KD or KV.

Fig. 5. Pheromone genes of *C. austroafricana*, *C. cubensis* and *C. deuterocubensis*. (A) Sequence alignment of the mature PPG1-1 peptide with the number of peptide repeats shown as grey and black rectangles. In cases where peptide sequences were different, the grey and black rectangles correspond to peptide sequences circled with a grey and black outline, respectively. (B) Alignment of the putative pheromone PPG2-1, PPG2-2 and PPG2-3 protein sequences. C and D show neighbor joining trees of all predicted pheromone genes using nucleotide and amino acid sequences, respectively. CC, CD and CA denote *C. cubensis*, *C. deuterocubensis* and *C. austroafricana*. The * and † denote sequences from the *MAT1-2* and *MAT1-1* isolates of *C. austroafricana*.

Three ORFs homologous to *C. parasitica Mf2/1* and *Mf2/2* (encoding the a-like pheromone) were identified from the genomes of *C. austroafricana*, *C. cubensis* and *C. deuterocubensis*. These ORFs were homologs of *ppg2* of other *Sordariomycetes* and were named *ppg2-1*, *ppg2-2* and *ppg2-3*. Unlike the *Mf2/1* and *Mf2/2* genes of *C. parasitica*, which are identical, each of the three genes of *C. austroafricana*, *C. cubensis* and *C. deuterocubensis* encoded unique sequences. The putative *ppg2-1* amino acid sequences of *C. austroafricana* (scaffold6; position 942102-942034), *C. cubensis* (scaffold_0047; LJCY01000146.1; position 44353-44421) and *C. deuterocubensis* (tig0010; position 643852-643784) were 23 residues long and shared 100% sequence identity with protein sequences *Mf2/1* and *Mf2/2* of *C. parasitica*. The inferred amino acid sequences of putative *ppg2-2* of *C. austroafricana* (scaffold9; position 1969827-1969759), *C. cubensis* (scaffold_0039; LJCY01000139.1; position 16886-16954) shared 82% sequence identity with *Mf2/1* of *C. parasitica*. In *C. deuterocubensis* a sequence in tig0007

19

position 132911-132982 shared 93% with the putative *ppg2-2* of *C. cubensis*. However, the CAAX motif could not be predicted thus, this sequence could not be considered as *ppg2* pheromone. The predicted amino acid sequences of the putative *ppg2-3* of *C. austroafricana* (scaffold10; position 507556-507624), *C. cubensis* (scaffold_0042; LJCY01000142.1; position 163149-163217) and *C. deuterocubensis* (tig0011; position 973020-973091) shred 78%, sequence identity with the *Mf2/1* of *C. parasitica*. Among the *Chrysoporthe* species, putative *ppg2-1* amino acid sequences shared 91% and 73% identity with the putative *ppg2-2* and *ppg2-3* respectively. The putative *ppg2-2* of *C. austroafricana MAT1-2* and *MAT1-1* isolates were absolutely conserved, but shared 91% sequence identity with the putative *ppg2-2* of *C. cubensis*. BLASTp comparison between putative *ppg2-2* of *C. austroafricana* and *ppg2-3* of *C. cubensis* and *C. deuterocubensis* revealed sequence identities ranging from 60% to 65%. However, the putative *ppg2-2* of *C. cubensis* shared sequence identity ranging from 69% to 73% with the *ppg2-3* of *C. cubensis*, *C. austroafricana* and *C. deuterocubensis*. Overall, the putative *ppg2-2* sequences showed higher percentages of sequence identity with *ppg2-1* than with *ppg2-3*.

Phylogenetic analyses using distance based methods clustered the putative *ppg1-1*, *ppg2-2* and *ppg2-3* genes separately. The putative a-like pheromones contained the C-terminal CAAX motif, which is also present in pheromones of other ascomycetes (Mayrhofer and Pöggeler 2005; Seibel *et al.* 2012; Zhang *et al.* 1998). The CAAX motif is comprised of a Cysteine (C), two aliphatic amino acids (AA) and any amino acid at the terminus of the sequence (X). The *ppg2-1* and *ppg2-3* pheromones contained two valine residues at the aliphatic positions, and a methionine at the terminus, thus forming the CVVM motif. On the other hand, *ppg2-2* contained isoleucine at the aliphatic positions, resulting in the pattern CIIM (Fig. 5B). The genomic locations of the three *ppg2* homologs of *Chrysoporthe* suggest that they are encoded from independent loci. Characterization of the genes flanking the putative *ppg2* ORFs revealed that *ppg2-1* was located adjacent to a gene encoding cyanate lyase, similar to *ppg2* of *Neurospora crassa*, *Magnaporthe grisea*, and *Gibberella zeae* (Lee *et al.* 2008). Homologs of cyanate lyase were not identified in either flanks of putative *ppg2-2* and *ppg2-3* genes. Also, microsyntenic conservation was not observed in the genomic loci containing the putative *ppg2-2* and *ppg2-3* genes. Consequently, we hypothesize that *ppg2-2* and *ppg2-3* are not orthologs of *ppg2-1*, but could rather be paralogs.

3.5.2. pre-1 and pre-2

ORFs encoding protein sequences containing transmembrane domains were identified in each of the genome sequences of *C. austroafricana*, *C. cubensis* and *C. deuterocubensis*. Out of these sequences, only two ORFs encoded protein sequences homologous to the STE3 (InterPro term IPR001499) and STE2 (InterPro term IPR000366) mating pheromone receptors. The putative pheromone receptor genes of *C. austroafricana*, *C. cubensis* and *C. deuterocubensis* were named *pre-1* and *pre-2*, in accordance with the convention in other filamentous ascomycetes (Kim and Borkovich 2004; Mayrhofer et al. 2006). The putative *pre-1* genes were 1,905 bp long in all three species and contained three introns (56 bp, 160 bp and 54 bp) at conserved positions. The size of *pre-2* was 1,339 bp in *C. austroafricana*, and 1,315 bp in *C. cubensis* and *C. deuterocubensis*. The putative *pre-2* gene in all three species contained only one intron (61 bp) located at a conserved site. Analysis of the inferred amino acid sequences PRE-1 (544 amino acid sequences in all three species) and PRE-2 (418 amino acids in *C. cubensis*, *C. deuterocubensis* and 426 amino acid sequences in *C. austroafricana*) showed that both contained seven transmembrane regions, interspersed between intracellular and extracellular loops. Multiple sequence alignment of the inferred PRE-1 and partial PRE-2 protein sequences revealed an average of 98% interspecific sequence identity.

3.6. Transcription analysis of *MAT1*, pheromone and receptor genes

Results from the RT-qPCR did not show significant differences ($p < 0.05$) in the expression of *ppg1* and *ppg2* in the *MAT1-2* and *MAT1-1* individuals (CMW2113 and CMW6102, respectively) of *C. austroafricana* (Fig. 6). However, the expression of *ppg1* was significantly different from that of *ppg2-1* in the homothallic *C. cubensis* isolate (CMW10028). In all three isolates the expression of *pre-1* and *pre-2* differed significantly (Fig. 6). In both *C. austroafricana* CMW2113 (*MAT1-1*) and *C. austroafricana* CMW6102 (*MAT1-2*), the expression of *pre-1* was slightly lower but not statistically different to that of *ppg1* and *ppg2*. In terms of the mating-type genes of the *MAT1-2* individual of *C. austroafricana*, the expression of *MAT1-1-2* was significantly lower than that of *MAT1-2-1* (Fig. 6). In the *MAT1-1* individual, *MAT1-1-2* was significantly more highly expressed than *MAT1-1-1* and *MAT1-1-3*.
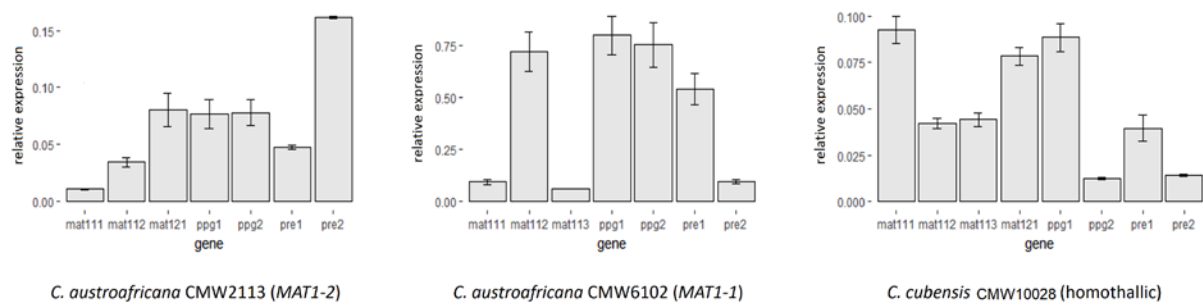
Fig. 6. Relative expression of pheromone genes, pheromone receptor genes and mating-type genes of *C. austroafricana* CMW2113 (*MAT1-2*), *C. austroafricana* CMW6102 (*MAT1-1*) and homothallic *C. cubensis* CMW10028. The expression level is relative to the level of the reference (actin) gene (=1). Letters below or above the box plots represent statistically significant differences in the gene expression levels at $p < 0.05$ between genes using the Tukey test.

In the homothallic *C. cubensis* isolate (CMW10028), the expression of *MAT1-1-2* and *MAT1-1-3* was comparable, as was the expression of *MAT1-1-1* and *MAT1-2-1*. The expression of *MAT1-1-1* and *MAT1-2-1* genes was significantly higher than that of *MAT1-1-2* and *MAT1-1-3* (Fig. 6). In the two individuals of *C. austroafricana*, expression of the pheromone receptor genes seemed to correlate with mating-type. In the *MAT1-2* individual with its highly expressed *MAT1-2-1* gene, *pre-2* was more highly expressed than *pre-1*. Also, in the *MAT1-1* individual, the high expression of *MAT1-1-2* matched the higher expression of *pre-1*. A similar trend was not observed for the pheromone genes, as both were expressed at relatively high levels in the two *MAT1-2* and *MAT1-1* isolates of *C. austroafricana*. In the homothallic *C. cubensis* isolate, the higher expression of *pre-1* and *ppg1-1* correlated with the higher expression levels of the *MAT1-1-1* and *MAT1-2-1* genes. However, this expression pattern did not correlate with the proposed pheromone-receptor pair *ppg1/pre-2* and *ppg2/pre-1* (Mayrhofer and Pöggeler, 2005).

4. Discussion

To date, the widely accepted hypothesis (Hodges et al., 1976; Hodges et al., 1979) regarding the mating system of *Chrysoporthe* species has been homothallism. This study is the first to provide concrete experimental evidence regarding the mating systems of *Chrysoporthe* species. This was achieved by identifying and characterizing the mating-type gene sequences of these species. *MAT loci* corresponding to *MAT1-1* and *MAT1-2* idiomorphs were identified in *C.*

austroafricana isolates CMW6102 and *C. austroafricana* CMW2113 respectively, suggesting that heterothallism is the mating system in this species. This result corroborates the rare occurrence of perithecia of *C. austroafricana* on Eucalyptus cankers (Nakabonge et al., 2006; Wingfield et al., 1989).

All *MAT* genes identified in the *MAT1-1* and *MAT1-2* idiomorphs of *C. austroafricana* were present in the genomes of both *C. cubensis* and *C. deuterocubensis*. This was consistent with the *MAT loci* of homothallic fungi (Debuchy and Turgeon, 2006). These results also corroborated previous laboratory experiments in which single ascospore cultures of *C. cubensis* could reproduce sexually without a compatible partner (Van der Merwe 2000). Also, our results could explain the prevalence of sexual fruiting bodies on the surfaces of cankers caused by *C. cubensis* and *C. deuterocubensis* (Gryzenhout et al., 2004; Myburg et al., 2003; Nakabonge et al., 2006). Put together, these results confirm that homothallism is the mating system of *C. cubensis* and *C. deuterocubensis*.

The presence of *MAT* genes as predicted from the identified mating-type loci of *C. austroafricana*, *C. cubensis* and *C. deuterocubensis* were confirmed by amplification of portions of these genes using PCR. All four *MAT* genes identified in this study were amplified in *C. cubensis* and *C. deuterocubensis,* confirming that these two species exhibit a homothallic mating system. In a randomly mating population, the expected ratio of mating types is even (Groenewald et al., 2006). From our analysis of 65 randomly selected *C. austroafricana* isolates, we confirmed the presence of two mating types based on the predicted structural organization of the *MAT1-1* and *MAT1-2* idiomorphs identified from the respective genome sequences. Our analysis showed that *MAT1-2* idiomorphs were more frequently encountered. However, skewed mating-type ratios in populations of *C. austroafricana* could explain the common occurrence of pycnidial (asexual) cankers on *Eucalyptus* spp., while perithecia are rare (Nakabonge et al., 2006).

In heterothallic species, the expression of pheromone and receptor genes is generally mating-type specific (Bobrowicz et al., 2002; Kim and Borkovich, 2006). Results from our expression analyses revealed that putative pheromone receptor genes *pre-1* and *pre-2* were transcribed in a mating-type dependent manner in both *C. austroafricana MAT1-1* and *MAT1-2* isolates. In contrast, the expression levels of putative pheromone genes *ppg1* and *ppg2* in both mating-types were similar and did not seem to be under the influence of the mating-type locus. This observation may be different during the sexual phase, although the expression of pheromone and pheromone receptor genes in heterothallic *Hypocrea jeronica* (*Trichoderma reesei*) do not

appear to be strictly mating-type dependent (Seibel et al., 2012). The expression of pheromones in heterothallic *C. austroafricana* during the vegetative phase could be indicative of pleiotropic functions, such as in *Neurospora crassa* (Kim et al., 2002).

The expression of pheromone genes (*ppg1*, *ppg2*) and pheromone receptor genes (*pre-1*, *pre-2*) in homothallic *C. cubensis* did not seem to follow the mating-type dependent expression pattern observed in heterothallic fungi. The expression of *ppg1* and *pre-1* was significantly different to that of *ppg2* and *pre2*. A mating-type dependent expression would have showed one of the cognate pheromone/receptor pairs *ppg1*/*pre-2* or *ppg2*/*pre-1* (Kim et al., 2012; Mayrhofer and Pöggeler, 2005) being significantly expressed. The non-mating-type specific expression pattern of pheromone genes and pheromone receptor genes in *C. cubensis* agreed with the expression pattern of these genes in other homothallic ascomycetes, such as *S. macrospora* (Mayrhofer and Pöggeler, 2005) and *G. zeae* (Kim et al., 2008; Lee et al., 2008). Overall, the expression profiles of pheromone and pheromone receptor genes in *C. austroafricana* and *C. cubensis* were congruent with heterothallism and homothallism in these species, respectively.

An interesting finding was the unique organization of the *MAT loci* of *Chrysoporthe austroafricana*. The *C. austroafricana MAT1-2* locus contained a truncated *MAT1-1-1* gene and an intact *MAT1-1-2* gene, unlike typical *MAT1-2* loci which contain *MAT1-2-1* only. The presence of *MAT1-1-2* gene in the *MAT1-2* locus has been recently reported in *Thielaviopsis* (Wilken et al., 2018). ORFs homologous to *MAT1-1-1* containing truncated MAT1-1-1 alpha-box domains were observed in the *MAT1-1-1* gene of *Diaporthe ampelina* (Morales-Cruz et al., 2015), as well as in the *MAT1-2* idiomorphs of *Leptographium procerum* and *L. profanum* (Duong et al., 2013). The *MAT1-2* locus of *Diaporthe* spp. does not contain a *MAT1-1-1* gene, but other genes associated with the *MAT1-1* locus have been identified. Thus, the authors speculated that this could be the ancestral structure and organization of *MAT1-2* loci of *Sordariomycetes* (Kanematsu et al., 2007).

The *MAT* locus of *C. deuterocubensis, C. cubensis* and *C. austroafricana* CMW2113 (MAT1-2) idiomorph contained ORFs homologous to long terminal repeat (LTR) retrotransposons. We hypothesize that *MAT1-2* and *MAT1-1* idiomorphs of *C. austroafricana* evolved from a homothallic ancestor in a mechanism that involved gene loss mediated by retrotransposons (Fig. 7). In this case, the *MAT1-2-1* and *MAT1-1-3* respectively were deleted from the *MAT* locus of the homothallic ancestor, resulting in the extant *MAT1-1* and *MAT1-2* idiomorphs of *C. austroafricana*. However, based on the placement of *C. austroafricana* in the reference

phylogenetic tree and the unusual positioning of *MAT1-1-2* after the *APN2*, it is possible that homothallism could have evolved from a heterothallic ancestor through unequal recombination. The role of repeat sequences in the evolution of the mating-type locus has been reported fungi such as *Sclerotinia trifoliorum* (Xu et al., 2016) and *Ceratocystis fimbriata* (Wilken et al., 2014) where they have been implicated in unidirectional mating type switching and repeat induced recombination in *Saccharomyces cerevisiae* (Hanson et al., 2014). Similarly, the role of LTRs in the evolution of mating systems has been reported in *Neurospora* species (Gioti et al., 2012). Additional whole genome sequences from other *Chrysoporthe* species are required for further studies aimed at establishing the evolutionary histories of *MAT* loci in these species and the molecular mechanisms involved.
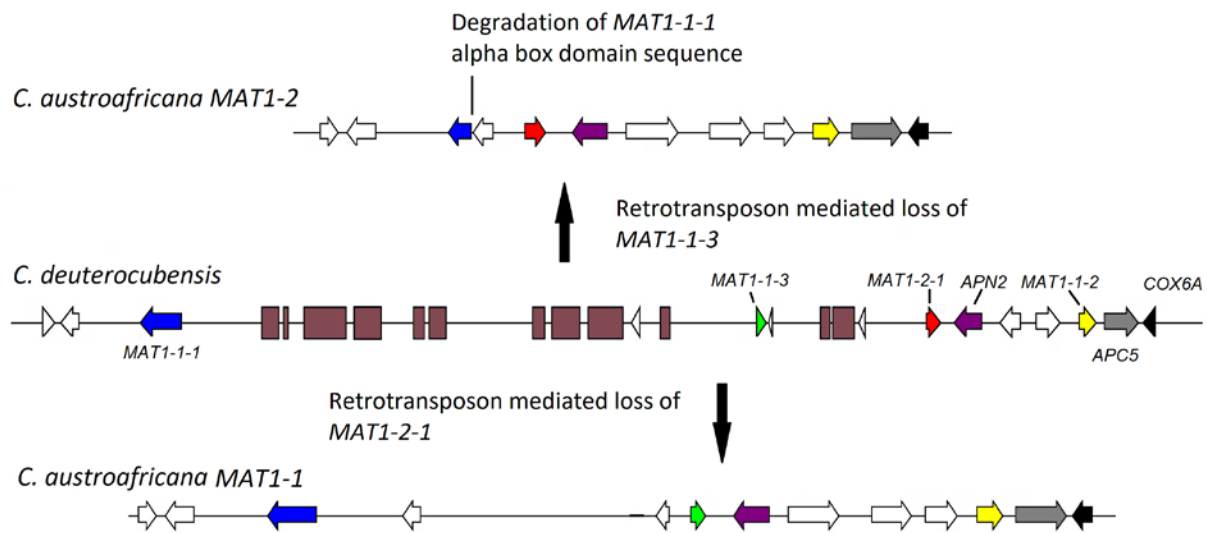
Fig. 7. Proposed evolution of the *C. austroafricana MAT* loci from a hypothetical homothallic ancestor through retrotransposon mediated gene loss of either *MAT1-2-1* as in the *MAT1-1* idiomorph or *MAT1-1-3* followed by degradation of the *MAT1-1-1* gene as shown in the *MAT1-2* idiomorph.

The availability of whole genome sequences enabled the identification of mating-type genes of *Chrysoporthe* species, thus providing the genetic basis for sexual reproduction and confirming observations from previous studies. We have determined that *C. austroafricana* is heterothallic and that *C. cubensis* and *C. deuterocubensis* are homothallic. However, further studies are required to fully understand the distribution of mating-types in natural populations, which is now possible using primers designed in the current study. Additionally, the specific functions of *MAT* genes in growth and development, and the role of mating-types in shaping the evolution of *C. austroafricana* and related species, can now be investigated.

Acknowledgements

References

Altschul, S.F., Gish, W., Miller, W., Myers, E.W., Lipman, D.J., 1990. Basic local alignment search tool. J. Mol. Biol. 215, 403-410.

Bidard, F., Benkhali, JA., Coppin, E., Imbeaud, S., Grognet, P., Delacroix, H., Debuchy, R., 2011. Genome-wide gene expression profiling of fertilization competent mycelium in opposite mating types in the heterothallic fungus *Podospora anserina*. PLoS One. 6, e21476.

Bihon, W., Wingfield, M.J., Slippers, B., Duong, T.A., Wingfield, B.D., 2014. *MAT* gene idiomorphs suggest a heterothallic sexual cycle in a predominantly asexual and important pine pathogen. Fungal Genet. Biol. 62, 55-61.

Blanco-Ulate, B., Rolshausen, P., Cantu, D., 2013. Draft genome sequence of the ascomycete *Phaeoacremonium aleophilum* strain UCR-PA7, a causal agent of the esca disease complex in grapevines. Genome Announc. 1, e00390-13.

Bobrowicz, P., Pawlak, R., Correa, A., Bell-Pedersen, D., Ebbole, D.J., 2002. The *Neurospora crassa* pheromone precursor genes are regulated by the mating type locus and the circadian clock. Mol. Microbiol. 45, 795-804.

Boetzer, M., Henkel, C.V., Jansen, H.J., Butler, D., Pirovano, W., 2011. Scaffolding pre-assembled contigs using SSPACE. Bioinformatics. 27, 578-9.

Capella-Gutierrez, S., Silla-Martinez, J.M., Gabaldon, T., 2009. trimAl: a tool for automated alignment trimming in large-scale phylogenetic analyses. Bioinformatics. 25, 1972-1973.

Conradie, E., Swart, W., Wingfield, M., 1990. Cryphonectria canker of Eucalyptus, an important disease in plantation forestry in South Africa. South For. 152, 43-49.

Coppin, E., Debuchy, R., Arnaise, S., Picard, M., 1997. Mating types and sexual development in filamentous ascomycetes. Microbiol. Mol. Biol. Rev. 61, 411-28.

Debuchy, R., Turgeon, B.G., 2006. Mating-type structure, evolution, and function in euascomycetes. In: U. Kües, R. Fischer, Eds.), Growth, differentiation and sexuality. Springer Berlin Heidelberg, pp. 293-323.

Debuchy, R., Berteaux-Lecellier, V., Silar, P., 2010. Mating systems and sexual morphogenesis in ascomycetes. In Cellular and molecular biology of filamentous fungi. American Society of Microbiology, Washington, DC ,pp. 501-535.

Duong, T.A., de Beer, Z.W., Wingfield, B.D., Wingfield, M.J., 2013. Characterization of the mating-type genes in *Leptographium procerum* and *Leptographium profanum*. Fungal Biol. 117**,** 411-421.

Dyer, P.S., Paoletti, M., 2005. Reproduction in *Aspergillus fumigatus*: sexuality in a supposedly asexual species? Med. Mycol. 43**,** 7-14.

Dyer, P.S., Paoletti, M., Archer, D.B., 2003. Genomics reveals sexual secrets of *Aspergillus*. Microbiology. 149**,** 2301-2303.

Galagan, J.E., Calvo, S.E., Cuomo, C., Ma, L.J., Wortman, J.R., Batzoglou, S., Lee, S.I., Basturkmen, M., Spevak, C.C., Clutterbuck, J., Kapitonov, V., Jurka, J., Scazzocchio, C., Farman, M., Butler, J., Purcell, S., Harris, S., Braus, G.H., Draht, O., Busch, S., D'Enfert, C., Bouchier, C., Goldman, G.H., Bell-Pedersen, D., Griffiths-Jones, S., Doonan, J.H., Yu, J., Vienken, K., Pain, A., Freitag, M., Selker, E.U., Archer, D.B., Penalva, M.A., Oakley, B.R., Momany, M., Tanaka, T., Kumagai, T., Asai, K., Machida, M., Nierman, W.C., Denning, D.W., Caddick, M., Hynes, M., Paoletti, M., Fischer, R., Miller, B., Dyer, P., Sachs, M.S., Osmani, S.A., Birren, B.W., 2005. Sequencing of *Aspergillus nidulans* and comparative analysis with *A. fumigatus* and *A. oryzae*. Nature. 438**,** 1105-15.

Gioti, A., Mushegian, A.A., Strandberg, R., Stajich, J.E., Johannesson, H., 2012. Unidirectional evolutionary transitions in fungal mating systems and the role of transposable elements. Mol. Biol. Evol. 29**,** 3215-3226.

Glass, N.L., Smith, M.L., 1994. Structure and function of a mating-type gene from the homothallic species *Neurospora africana*. Mol. Gen. Genet. 244, 401–409.

Groenewald, M., Groenewald, J.Z., Harrington, T.C., Abeln, E.C., Crous, P.W., 2006. Mating type gene analysis in apparently asexual *Cercospora* species is suggestive of cryptic sex. Fungal Genet. Biol. 43**,** 813-825.

Gryzenhout, M., Myburg, H., Van der Merwe, N.A., Wingfield, B.D., Wingfield, M.J., 2004. *Chrysoporthe*, a new genus to accommodate *Cryphonectria cubensis*. Studies In Mycology. 50**,** 119–142.

Haber, J.E., 2012. Mating-Type Genes and *MAT* Switching in *Saccharomyces cerevisiae*. Genetics. 191**,** 33-64.

Hanson, S.J., Byrne, K.P., Wolfe, K.H., 2014. Mating-type switching by chromosomal inversion in methylotrophic yeasts suggests an origin for the three-locus *Saccharomyces cerevisiae* system. Proceedings of the National Academy of Sciences. 111**,** E4851-E4858.

Heath, R.N., Gryzenhout, M., Roux, J., Wingfield, M.J., 2006. Discovery of the canker pathogen *Chrysoporthe austroafricana* on native *Syzygium* spp. in South Africa. Plant Dis. 90**,** 433-438.

Hodges, C., Reis, M., Ferreira, F., Henfling, J., 1976. O cancro do Eucalipto causado por *Diaporthe cubensis* [*Eucalyptus* spp.; Fungo; Brasil]. Fitopatologia Brasileira. 1**,** 129-170.

Hodges, C.S., Geary, T.F., Cordell, C.E., 1979. The occurrence of *Diaporthe cubensis* on Eucalyptus in Florida, Hawaii, and Puerto Rico. Plant Disease Reporter. 63**,** 216-220

Hujslová, M., Kubátová, A., Kostovčík, M., Blanchette, R.A., de Beer, Z.W., Chudíčková, M., Kolařík, M., 2014. Three new genera of fungi from extremely acidic soils. Mycol Progress. 13**,** 819-831.

Inderbitzin, P., Berbee, M.L., 2001. Lollipopaia minuta from Thailand, a new genus and species of the *Diaporthales* (Ascomycetes, Fungi) based on morphological and molecular data. Can J Bot. 79**,** 1099-1106.

Kanamori, M., Kato, H., Yasuda, N., Koizumi, S., Peever, T.L., Kamakura, T., Teraoka, T., Arie, T., 2007. Novel mating type-dependent transcripts at the mating type locus in *Magnaporthe oryzae*. Gene. 403**,** 6-17.

Kanematsu, S., Adachi, Y., Ito, T., 2007. Mating-type loci of heterothallic *Diaporthe* spp.: homologous genes are present in opposite mating-types. Curr. Genet. 52**,** 11-22.

Katoh, K., Misawa, K., Kuma, K.i., Miyata, T., 2002. MAFFT: A novel method for rapid multiple sequence alignment based on fast Fourier transform. Nucleic Acids Res. 30**,** 3059-3066.

Kim, H., Borkovich, K.A., 2004. A pheromone receptor gene, *pre-1*, is essential for mating type-specific directional growth and fusion of trichogynes and female fertility in *Neurospora crassa*. Mol. Microbiol. 52**,** 1781-1798.

Kim, H., Borkovich, K.A., 2006. Pheromones are essential for male fertility and sufficient to direct chemotropic polarized growth of trichogynes during mating in *Neurospora crassa*. Eukaryot. Cell. 5**,** 544-554.

Kim, H., Metzenberg, R.L., Nelson, M.A., 2002. Multiple functions of *mfa-1*, a putative pheromone precursor gene of *Neurospora crassa*. Eukaryot. Cell. 1**,** 987-999.

Kim, H., Wright, S.J., Park, G., Ouyang, S., Krystofova, S., Borkovich, K.A., 2012. Roles for receptors, pheromones, G proteins, and mating type genes during sexual reproduction in *Neurospora crassa*. Genetics. 190**,** 1389-1404.

Kim, H.K., Lee, T., Yun, S.H., 2008. A putative pheromone signaling pathway is dispensable for self-fertility in the homothallic ascomycete *Gibberella zeae*. Fungal Genet. Biol. 45**,** 1188-1196.

Kohany, O., Gentles, A. J., Hankus, L., & Jurka, J., 2006. Annotation, submission and screening of repetitive elements in Repbase: RepbaseSubmitter and Censor. BMC Bioinformatics, 7, 474.

Koren, S., Walenz, B.P., Berlin, K., Miller, J.R., Bergman, N.H., Phillippy, A.M., 2017. CANU: Scalable and accurate long-read assembly via adaptive k-mer weighting and repeat separation. Genome Res. 27, 722-736.

Kronstad, J.W., Staben, C., 1997. Mating type in filamentous fungi. Annual Reviews of Genetics. 31**,** 245-276.

Lamprecht, S.C., Crous, P.W., Groenewald, J.Z., Tewoldemedhin, Y.T., Marasas, W.F., 2011. *Diaporthaceae* associated with root and crown rot of maize. IMA Fungus. 2**,** 13-24.s

Lee, J., Leslie, J.F., Bowden, R.L., 2008. Expression and function of sex pheromones and receptors in the homothallic ascomycete *Gibberella zeae*. Eukaryot. Cell. 7**,** 1211-1221.

Li, S., Song, Q., Ji, P., Cregan, P., 2015. Draft genome sequence of *Phomopsis longicolla* type strain TWH P74, a fungus causing phomopsis seed decay in soybean. Genome Announc. 3**,** e00010-15

Li, W., Sullivan, T.D., Walton, E., Averette, A.F., Sakthikumar, S., Cuomo, C.A., Klein, B.S., Heitman, J., 2013. Identification of the mating-type *(MAT)* locus that controls sexual reproduction of *Blastomyces dermatitidis*. Eukaryot. Cell. 12**,** 109-117.

Marra, R.E., Cortesi, P., Bissegger, M., Milgroom, M.G., 2004. Mixed mating in natural populations of the chestnut blight fungus, *Cryphonectria parasitica*. Heredity. 93**,** 189-195.

Mayrhofer, S., Pöggeler, S., 2005. Functional characterization of an α-factor-like *Sordaria macrospora* peptide pheromone and analysis of its interaction with its cognate receptor in *Saccharomyces cerevisiae*. Eukaryot. Cell. 4**,** 661-672.

Mayrhofer, S., Weber, J.M., Pöggeler, S., 2006. Pheromones and pheromone receptors are required for proper sexual development in the homothallic ascomycete *Sordaria macrospora*. Genetics. 172**,** 1521-1533.

Merino, S.T., Nelson, M.A., Jacobson, D.J., Natvig, D.O., 1996. Pseudohomothallism and evolution of the mating-type chromosome in *Neurospora tetrasperma*. Genetics. 143**,** 789-799.

Metzenberg, R., Glass, N., 1990. Mating type and mating strategies in *Neurospora*. Bioessays. 12**,** 53 - 59.

Morales-Cruz, A., Amrine, K.C.H., Blanco-Ulate, B., Lawrence, D.P., Travadon, R., Rolshausen, P.E., Baumgartner, K., Cantu, D., 2015. Distinctive expansion of gene families associated with plant cell wall degradation, secondary metabolism, and nutrient uptake in the genomes of grapevine trunk pathogens. BMC Genomics. 16**,** 1-22.

Myburg, H., Gryzenhout, M., Wingfield, B.D., Wingfield, M.J., 2002. β-Tubulin and histone H3 gene sequences distinguish *Cryphonectria cubensis* from South Africa, Asia, and South America. Can J Bot. 80**,** 590-596.

Myburg, H., Gryzenhout, M., Wingfield, B.D., Wingfield, M.J., 2003. Conspecificity of *Endothia eugeniae* and *Cryphonectria cubensis*: a re-evaluation based on morphology and DNA sequence data. Mycoscience. 44**,** 187-196.

Nakabonge, G., Roux, J., Gryzenhout, M., Wingfield, M.J., 2006. Distribution of Chrysoporthe canker pathogens on *Eucalyptus* and *Syzygium* spp. in eastern and southern Africa. Plant Dis. 90**,** 734-740.

Nygren, K., Strandberg, R., Gioti, A., Karlsson, M., Johannesson, H., 2012. Deciphering the relationship between mating system and the molecular evolution of the pheromone and receptor genes in *Neurospora*. Mol. Biol. Evol. 29**,** 3827-3842.

Peng, Y., Leung, H.C., Yiu, S.M., Chin, F.Y., 2012. IDBA-UD: A *de novo* assembler for single-cell and metagenomic sequencing data with highly uneven depth. Bioinformatics. 28**,** 1420-1428.

Pöggeler, S., 2000. Two pheromone precursor genes are transcriptionally expressed in the homothallic ascomycete *Sordaria macrospora*. Curr. Genet. 37**,** 403-411.

Rodas, C.A., Gryzenhout, M., Myburg, H., Wingfield, B.D., Wingfield, M.J., 2005. Discovery of the Eucalyptus canker pathogen *Chrysoporthe cubensis* on native Miconia (Melastomataceae) in Colombia. Plant Pathol. 54**,** 460-470.

Rydholm, C., Dyer, P.S., Lutzoni, F., 2007. DNA Sequence characterization and molecular evolution of *MAT1* and *MAT2* Mating-type loci of the self-compatible ascomycete mold *Neosartorya fischeri*. Eukaryot. Cell. 6**,** 868-874.

Schmittgen, T.D., Livak, K.J., 2008. Analyzing real-time PCR data by the comparative CT method. Nat. Protocols. 3**,** 1101-1108.

Seibel, C., Tisch, D., Kubicek, C.P., Schmoll, M., 2012. The role of pheromone receptors for communication and mating in *Hypocrea jecorina* (*Trichoderma reesei*). Fungal Genet. Biol. 49**,** 814-824.

Simão, F.A., Waterhouse, R.M., Ioannidis, P., Kriventseva, E.V., Zdobnov, E.M., 2015. BUSCO: assessing genome assembly and annotation completeness with single-copy orthologs. Bioinformatics. btv351.

Stamatakis, A., 2014. RAxML version 8: A tool for phylogenetic analysis and post-analysis of large phylogenies. Bioinformatics. 30**,** 1312-1313.

Stanke, M., Morgenstern, B., 2005. AUGUSTUS: A web server for gene prediction in eukaryotes that allows user-defined constraints. Nucleic Acids Res. 33**,** W465-W467.

Steenkamp, E., Wingfield, B., Coutinho, T., Wingfield, M., Marasas, W., 1999. Differentiation of *Fusarium subglutinans f.* sp. *pini* by histone gene sequence data. Appl. Environ. Microbiol. 65**,** 3401-3406.

Sullivan, M. J., Petty, N. K., & Beatson, S. A., 2011. Easyfig: a genome comparison visualizer. Bioinformatics. 27, 1009-10.

Turgeon, B.G., Yoder, O.C., 2000. Proposed nomenclature for mating type genes of filamentous ascomycetes. Fungal Genet. Biol. 31**,** 1-5.

Van der Merwe NA (2000) Molecular phylogeny and population biology studies on the eucalyptus canker pathogen Cryphonectria cubensis: Chapter 3 M.Sc. Thesis. Department of Genetics, Pretoria, South Africa: University of Pretoria.

Van der Merwe, N.A., Gryzenhout, M., Steenkamp, E.T., Wingfield, B.D., Wingfield, M.J., 2010. Multigene phylogenetic and population differentiation data confirm the existence of a cryptic species within *Chrysoporthe cubensis*. Fungal Biol. 114**,** 966-979.

Van Heerden, S.W., Wingfield, M.J., 2001. Genetic diversity of *Cryphonectria cubensis* isolates in South Africa. Mycol. Res. 105**,** 94-99.

Vermeulen, M., Gryzenhout, M., Wingfield, M.J., Roux, J., 2013. Population structure of *Chrysoporthe austroafricana* in southern Africa determined using Vegetative Compatibility Groups (VCGs). For. Pathol. 43**,** 124-131.

Walker, B.J., Abeel, T., Shea, T., Priest, M., Abouelliel, A., Sakthikumar, S., Cuomo, C.A., Zeng, Q., Wortman, J., Young, S.K., Earl, A.M., 2014. Pilon: An integrated tool for comprehensive microbial variant detection and genome assembly improvement. Plos One. 9**,** e112963.

Wendland, J., Dünkler, A., Walther, A., 2011. Characterization of α-factor pheromone and pheromone receptor genes of *Ashbya gossypii*. FEMS Yeast Res. 11**,** 418-429.

Wilken, P.M., Steenkamp, E.T., Wingfield, M.J., de Beer, Z.W., Wingfield, B.D., 2014. DNA loss at the *Ceratocystis fimbriata* mating locus results in self-sterility. PLoS One. 9**,** e92180.

Wilken, P.M., Steenkamp, E.T., Wingfield, M.J., De Beer, Z.W., Wingfield, B.D., 2017. Which *MAT gene*? Pezizomycotina (Ascomycota) mating-type gene nomenclature reconsidered. Fungal Biol. Rev. 31**,** 199-211.

Wilken, P. M., Steenkamp, E. T, Van der Nest M A., Wingfield, M. J., Z. De Beer, Z.W, Wingfield B.D., 2018. Unexpected placement of the MAT1-1-2 gene in the MAT1-2 idiomorph of *Thielaviopsis* Fungal Genet Biol.,10.1016/j.fgb.2018.01.007

Wilson, A.M., Godlonton, T., van der Nest, M.A., Wilken, P.M., Wingfield, M.J., Wingfield, B.D., 2015. Unisexual reproduction in *Huntiella moniliformis*. Fungal Genet. Biol. 80**,** 1-9.

Wingfield, B.D., Ades, P.K., Al-Naemi, F.A., Beirn, L.A., Bihon, W., Crouch, J.A., De Beer, Z.W., De Vos, L., Duong, T.A., Fields, C.J., Fourie, G., Kanzi, A.M., Malapi-Wight, M., Pethybridge, S.J., Radwan, O., Rendon, G., Slippers, B., Santana, Q.C., Steenkamp, E.T., Taylor, P.W.J., Vaghefi, N., Van der Merwe, N.A., Veltri, D., Wingfield, M.J., 2015a. IMA Genome-F 4. Draft genome sequences of *Chrysoporthe austroafricana, Diplodia scrobiculata*, *Fusarium nygamai*, *Leptographium lundbergii*, *Limonomyces culmigenus*, *Stagonosporopsis tanaceti*, and *Thielaviopsis punctulata*. IMA Fungus 6**,** 233-248.

Wingfield, B.D., Barnes, I., De Beer, Z.W., De Vos, L., Duong, T.A., Kanzi, A.M., Naidoo, K., Nguyen, H.D.T., Santana, Q.C., Sayari, M., Seifert, K.A., Steenkamp, E.T., Trollip, C., van der Merwe, N.A., van der Nest, M.A., Wilken, P.M., Wingfield, M.J., 2015b. IMA Genome-F 5: Draft genome sequences of *Ceratocystis eucalypticola*, *Chrysoporthe cubensis*, *C. deuterocubensis*, *Davidsoniella virescens*, *Fusarium*

temperatum, *Graphilbum fragrans*, *Penicillium nordicum*, and *Thielaviopsis musarum*. IMA Fungus. 6**,** 493-506.

Wingfield, M.J., 2003. Daniel McAlpine Memorial Lecture Increasing threat of diseases to exotic plantation forests in the southern hemisphere: lessons from Cryphonectria canker. Australas. Plant Pathol. 32**,** 133-139.

Wingfield, M.J., Swart, W.J., Abear, B.J., 1989. First Record of *Cryphonectria* Canker of *Eucalyptus* in South Africa. Phytophylactica. 20**,** 311-313.

Xu, L., Jardini, T.M., Chen, W., 2016. Direct repeat-mediated DNA deletion of the mating type *MAT1-2* genes results in unidirectional mating type switching in *Sclerotinia trifoliorum*. Scientific Reports. 6**,** 27083.

Yin, Z., Liu, H., Li, Z., Ke, X., Dou, D., Gao, X., Song, N., Dai, Q., Wu, Y., Xu, J.R., 2015. Genome sequence of Valsa canker pathogens uncovers a potential adaptation of colonization of woody bark. New Phytol. 208**,** 1202-1216.

Zhang, L., Baasiri, R.A., Van Alfen, N.K., 1998. Viral repression of fungal pheromone precursor gene expression. Mol. Cell. Biol. 18**,** 953-959.